Rev. Adv. Mater. Sci. 47 (2016) 16-25

MICROSTRUCTURE, STRENGTH, ELECTRICAL CONDUCTIVITY AND HEAT RESISTANCE OF AN Al-Mg-Zr ALLOY AFTER ECAP-CONFORM AND COLD DRAWING

M.Yu. Murashkin[1,2], A.E. Medvedev[1], V.U. Kazykhanov[1], G.I. Raab[1], I.A. Ovid'ko[3] and R.Z. Valiev[1,2,3]

[1]Institute of Physics of Advanced Materials, Ufa State Aviation Technical University, Ufa 450000, Russia
[2]Laboratory for Mechanics of Bulk Nanomaterials, Saint Petersburg State University, Saint-Petersburg 98504, Russia
[3]Peter the Great St. Petersburg Polytechnic University, Saint-Petersburg 195251, Russia

Received: October 14, 2016

Abstract. This paper describes the routes to process conducting materials based on the Al-Mg-Zr system combining high strength (UTS=267 MPa), electrical conductivity (over 57% IACS) and heat resistance (up to 150°C). These properties in the alloy with 0.4 wt.% Mg and 0.2 wt.% Zr are achieved through the formation of ultrafine-grained microstructure (UFG) by thermomechanical treatment (TMT), including annealing, severe plastic deformation (SPD) via equal channel angular pressing-Conform (ECAP-C) followed by cold drawing. The mechanical strength is enhanced by the formation of ultrafine grains during ECAP-C and their additional refinement through cold drawing. Also, ECAP-C and drawing result in the material strengthening due to increased dislocation density. The annealing of the alloy prior to SPD is used to provide a good heat resistance and high electrical conductivity via formation of nanoscale Al_3Zr metastable precipitates and, correspondingly decreasing the concentration of Zr atoms in the Al solid solution.

1. INTRODUCTION

Bare Aluminium Conductors Steel Reinforced (ACSR) are widely used for power transmission in overhead power lines [1,2]. However, lately All Aluminium Alloy Conductors (AAAC) made of heat hardenable Al-Mg-Si alloys like EN AW-6101 and EN-AW 6201 are considered as a possible alternative to ACSR [3-5]. As compared to conventional ACSR conductors, AAAC have superior corrosion resistance, better strength to weight ratio, higher current carrying capacity, enable simpler mounting, etc. [3]. In this regard, studies to enhance the properties of Al-Mg-Si alloys have received much consideration [4,6-10]. Recently, it has been found that a new approach proposed in [11-13] is more promising from the commercial point of view than the application of conventional techniques like modification of chemical composition and thermomechanical treatment (TMT) parameters to enhance the alloys' properties. As to the new approach, enhanced strength (UTS over 360 MPa) and electrical conductivity (over 56% IACS) are achieved through processing of controlled ultrafine grained (UFG) microstructure via special TMT including SPD process. AAAC conductors with such a level of properties become even more attractive for application in overhead power lines.

However, the main shortcoming of AAAC Al-Mg-Si conductors is that their maximum long-time operating temperature is only +90 °C. This

Corresponding author: M.Yu. Murashkin, e-mail: m.murashkin.70@gmail.com

Table 1. Chemical content of the Al alloy (wt.%).

Mg	Zr	Fe	Si	Zn	(ΣTi+V+Cr+Mn)	Al
0.40	0.20	≥0.10	≥0.05	≥0.05	≥0.015	99.20

considerably reduces the conductors' capacity due to the increased risk of strength degradation.

To increase the service temperature of conductors up to 150-230 °C [14], it is conventional to use Al-Zr alloys with Zr content from 0.10 to 0.20 wt.%, and in some cases above 0.3 wt.% [15-18]. Usually Al-Zr rods processed via combined casting and rolling prior to cold drawing are subjected to t heat treatment (HT) by annealing at 300-450 °C [16-19]. As a result, nanoscale Al_3Zr precipitates (metastable modification $L1_2$) are formed in Al matrix, which prevent microstructure degradation and accordingly preserve wire current-conducting properties at elevated operating temperatures. At the same time, higher thermal stability of Al-Zr alloys is accompanied by much lower strength (UTS from 159 to 248 MPa) as compared to Al-Mg-Si alloys [14]. Therefore, it seems particularly important to process Al alloys with enhanced strength, thermal stability as well as high conductivity suitable to produce AAAC conductors holding much promise for the industry.

This area of research has attracted a great interest in recent years. For example, in [20], the Al-Zr alloy additionally alloyed with Sc to 0.2 wt.% was proposed to be used as a conducting material with enhanced physical and mechanical properties. Semi-finished billets were processed with a specialized TMT and demonstrated a UTS of more than 210 MPa and electrical conductivity of ~ 60% IACS. In [19, 21], Al-based alloys containing Zr, Mn, Cu, and Si were subjected to a special TMT and cold drawing, which resulted in a UTS in the range of 275-320 MPa depending on the content of alloying elements. The further annealing at 180 °C for 400 hours had a little effect on the alloys' strength. At the same time, the obtained conducting materials have relatively low electrical conductivity (from 48 to 54% IACS), while the presence of copper requires close control over their corrosive resistance.

It is important to note that the promising mechanism to enhance both the mechanical properties and the electrical conductivity of conducting materials by formation of UFG microstructure was left outside the scope of all the above-mentioned studies. In a number of our recent publications, we have demonstrated both a considerable enhancement of mechanical properties and the possibility to efficiently control electrical resistivity and heat resistance as a result of UFG microstructure generated in conducting materials [22,23].

This paper presents the results of the first studies observing the possibility to process Al-based conducting materials with both enhanced strength (like Al-Mg-Si alloys) and high electrical conductivity, and heat resistance. A comprehensive approach covered in the study combines a careful selection of the alloy chemical composition and the formation of controlled UFG microstructure via TMT including SPD process.

2. MATERIAL AND EXPERIMENTAL PROCEDURES

The Al-Mg-Zr alloy in the form of rods 9.0 mm in diameter processed via continuous casting and rolling with a chemical composition shown in Table 1 was used as the material for investigation. The material for investigation was supplied by UC RUSAL (Moscow, Russia).

An UFG microstructure in the material under study was formed by equal channel angular pressing-Conform (ECAP-C). This SPD technique enables to process an UFG microstructure, considerably enhancing both mechanical and service properties in long-length rods made of Al and Ti alloys [13, 24-27], as well as in steels [28] as compared to similar semi-finished products processed conventionally. Besides, obtained rod billets can be easily transformed into wire via rolling to produce conductors, while their geometry enables to reliably characterize both mechanical and service properties of the material [14].

Prior to ECAP-C rods up to 1 m long were subjected to a specialized HT, namely annealing at 385 °C. According to [16-19, 21], annealing of Al-Zr alloys at the temperature up to 400 °C is the most efficient way to process nanoscale Al_3Zr precipitates the average size and volume fraction enough to suppress the degradation of microstructure and properties of Al alloys at elevated service temperature. Some other studies also noted that annealing at a temperature below 400 °C can somewhat enhance the strength of Al-Zr alloys

through the implementation of precipitation hardening mechanism [29, 30].

ECAP-C machine was used to process wire rods under isothermal conditions at room temperature (RT). Intersection angle of channels (Φ) constituted 120° at 5 mm/s ram speed with six processing cycles corresponding to an equivalent (Von Misses) strain of about 4 [31]. A wire rod was rotated around the axis by +90° after each ECAP-C cycle (route Bc). According to the previous studies [13,32,33], it is the most efficient mode to form a homogeneous UFG microstructure in Al alloys. ECAP-C treatment resulted in the production of rods up to 1 m in length with a square cross section of 8 × 8 mm.

Pilot wire samples 3.2 mm in diameter were processed via cold drawing from billets subjected to ECAP-C. Drawing resulted in the overall reduction of ~ 85%.

Microstructural studies were performed using transmission and scanning electron microscopy (TEM and SEM) techniques. TEM investigations were implemented using JEOL JEM-2100 electron microscope at an accelerating voltage of 200 kV. To study the microstructure, thin foils were produced by jet polishing on Tenupol-5 machine with the chemical solution consisting of 20% nitric acid and 80% methanol at a temperature of -25 °C and a voltage of 15 V. At least 200 grains were measured to determine a mean size of structural elements by Grain-Size software. At least three foils were studied per each state to obtain statistically reliable results.

The microstructure homogeneity as well as the distribution of particles of secondary phases were estimated by SEM using JEOL JSM-6490LV at an accelerating voltage of 20 kV. The SEM is equipped with the INCA X-sight attachment for energy dispersive X-ray (EDX) analysis.

X-ray studies were performed using Rigaku Ultima IV diffractometer by CuK_{α} irradiation (30 kV and 20 mA). The coherent scattering domain (CSD) size, values of mean-square microdistortion of crystalline lattice ($<\varepsilon^2>^{1/2}$) and a crystalline lattice parameter were calculated using Rietveld analysis with the help of MAUD software [34]. To estimate dislocation density (ρ), the outcomes of X-ray measurements were used [35].

The Vickers hardness (HV) was measured on a Micromet-5101 device with a diamond pyramid indenter, a load of 0.3 kg (~2.94 N) and a dwell time of 15 s. Data provided in the following sections are the average of at least 15 measurements.

Mechanical testing was performed at room temperature using Instron 5982 tensile testing machine at a strain rate of 10^{-3} s^{-1}. Strength (yield strength (YS) and ultimate tensile strength (UTS)) and ductility characteristics (elongation to failure (El.)) of rods were estimated based on tensile testing of the samples with a cylindrical gauge section having 3 mm in diameter and a length of 15 mm and wire samples with a gauge section length of 250 mm were subjected to tensile testing to measure their strength characteristics [14]. To obtain consistent results, at least three samples were tested per each data point.

Electrical resistivity of the material under study was measured in straightened samples of at least 1 m long in a measured part [14,36].

Heat resistance of wire was determined on the basis of UTS variation after annealing at 230 °C for 1 hour in accordance with [14].

3. RESULTS AND DISCUSSION

3.1. Selection of the alloy chemical composition

The alloying elements and their content in the material for investigation were selected based on the following requirements: (i) UFG microstructure shall be processed in the alloy via SPD to provide the necessary strength level; (ii) the alloy shall contain precipitates, and their size and volume fraction shall ensure the stability of the UFG microstructure preserving the strength of conductors at elevated service temperature; (iii) the UFG alloy solid solution shall contain a minimum number of alloying element atoms, which have a profound effect on the alloy electrical conductivity; (iv) the content of alloying elements shall not allow the formation of secondary phases, which have a notable effect on the alloy operating characteristics, including corrosion behavior at elevated temperature.

In this regard, Zr was selected as one of the alloying elements. As shown in earlier studies [16-18], the content of Zr shall be ≥0.2 wt.% to support the operation of Al-Zr conductors at a service temperature up to ≥150 °C. Also, in [16], it was found that the decrease in Zr content in Al solid solution down to 1 wt.% resulting from the formation of nanoscale Al_3Zr particles has only a slight effect on electrical resistivity and increases it only by 0.4 nΩm/%wt.

Mg was selected as the second alloying element, since its presence in Al alloys is well known to considerably decrease a grain average size during SPD [37-39] and, respectively, to notably enhance the strength of the material. Also, Al electrical resistance is almost unaffected by Mg concentration up to 1 wt.% (no more than by 5.6 nΩm, according

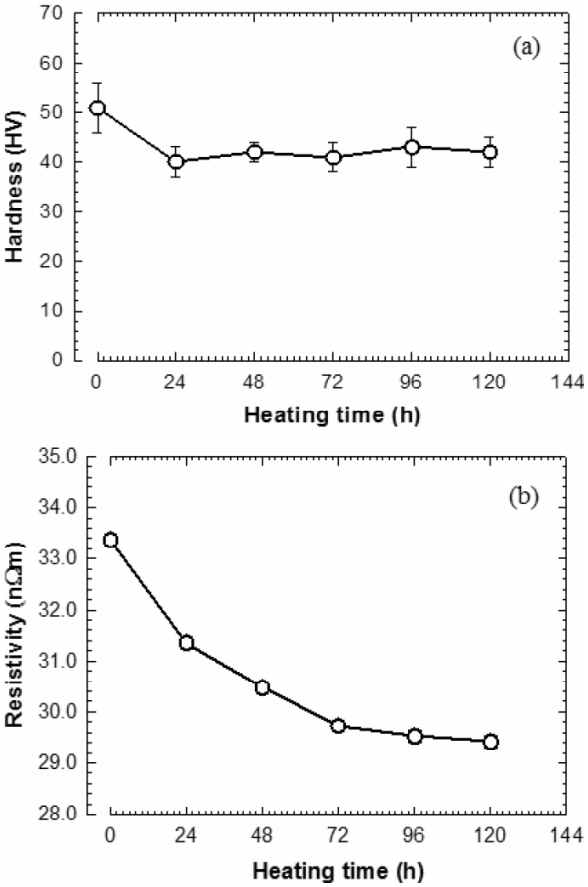

Fig. 1. Change in hardness and electrical resistivity of the as-received Al-0.4Mg-0.2Zr alloy after heat treatment at 385 °C over time.

to [40]). It is important to note that such a low Mg content in Al-Mg alloys has no effect on their corrosion behavior [41], which is of particular significance to conducting materials, especially bare conductors AAAC used in overhead power lines.

Based on this data, the content of Mg in the alloy under study was selected to be 0.4 wt.%, which doesn't exceed its equilibrium concentration in Al at room temperature [41]. At the same time, according to earlier studies [42,43], even lower Mg content results in the formation of UFG microstructure in ECAP-processed Al-Mg alloys with grains smaller than in CP Al. So, the selected Mg concentration shall lead to a considerable strengthening of the material in compliance with the Hall-Petch relationship [44,45], and have a little effect on electrical conductivity.

Another key factor taken into account when selecting alloying components is the absence of AlMgZr triple connections in Al-Mg-Zr alloys according to a phase diagram [46]. So, the selected concentration of Mg and Zr shall be preserved in Al-based solid solution processed by combined casting and rolling.

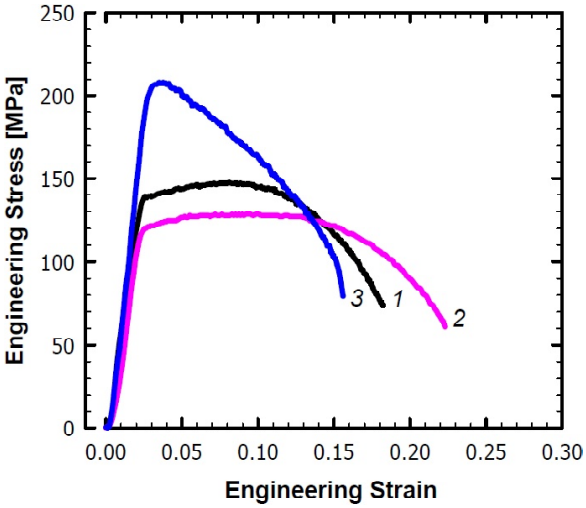

Fig. 2. Typical engineering stress—engineering strain curves from tensile testing of the Al-0.4Mg-0.2Zr alloy (1) in the initial state; (2) after heat treatment at 385 °C, 120 h; (3) after ECAP-C processing.

3.2 Properties and structure of the alloy following a heat treatment

Initial rods were subjected to a annealing at 385 °C to form nanoscale Al_3Zr precipitates, supporting the stability of an UFG microstructure at an elevated service temperature. The given microstructure was processed via ECAP-C and cold drawing. To find the most efficient duration of annealing, hardness and specific electrical resistivity (at 20 °C) of the material were measured each 24 hours of holding. Fig. 1 shows the variations in these characteristics against the annealing time.

It can be seen that a considerable decrease in the alloy hardness takes place after annealing for 24 hours (from 51±4 to 41±3 HV). Then it remains nearly the same till the end of the treatment (Fig. 1a). Specific electrical resistivity of the material, unlike the alloy hardness, decreases monotonically during annealing up to 72 hours (from 33.37 nΩm to 29.72 nΩm), and then changes only slightly comprising 29.42 nΩm (Fig. 1b) after annealing for 120 hours, which corresponds to 58.6% IACS.

The results of mechanical testing of the alloy processed by the HT are presented in Fig. 2 and Table 2, showing the loss in strength of the initial alloy after the treatment. The ductility of the alloy increases from 16.1 to 21.2%.

According to TEM studies, a structure with a subgrain size of about 4 μm was formed in initial billets produced by combined casting and rolling (Figs. 3a and 3b). This can be seen in selected area electron diffraction (SAED) patterns, one of

Table 2. Mechanical properties and electrical conductivity of the Al alloy.

State	YS, [MPa]	UTS, [MPa]	El, [%]	Resistivity at 20 °C, [nΩm]	IACS, [%]
Initial state	125±10	149±5	16.1±1.7	33.37	51.7
Heat treated (HT) – annealed at 385 °C, 120 h	85±8	129±5	21.2±0.9	29.42	58.6
HT + 6 passes ECAP-C at RT	188±13	205±9	14.6±0.7	29.93	57.6
5005-O (Al-0.8 wt.% Mg) [47]	45	125	25	-	-
Wire 3.2 mm in diameter produced from UFG rods					
ECAP-C + cold drawing	249±12	267±9	2.4±0.2	30.18	57.1
ECAP-C + cold drawing + anneal. at 230 °C, 1 h	222±11	245±8	3.3±0.3	30.09	57.3
Parameters of thermals resistant Al-Zr alloy wires					
AT1 [14]	-	159-169	≥2.0	28.735	60.0
AT2 [14]	-	225-248		31.347	55.0
AT3 [14]	-	159-176		28.735	60.0
AT4 [14]	-	159-169		29.726	58.0
Al-0.2Sc-0.04Zr [20]	-	213.3	-	-	61.7
Al-0.32...0.45Zr-0.16...0.56Mn-0.18...0.30Cu-0.18...0.25Si [19]	-	275-321	-	-	54-48

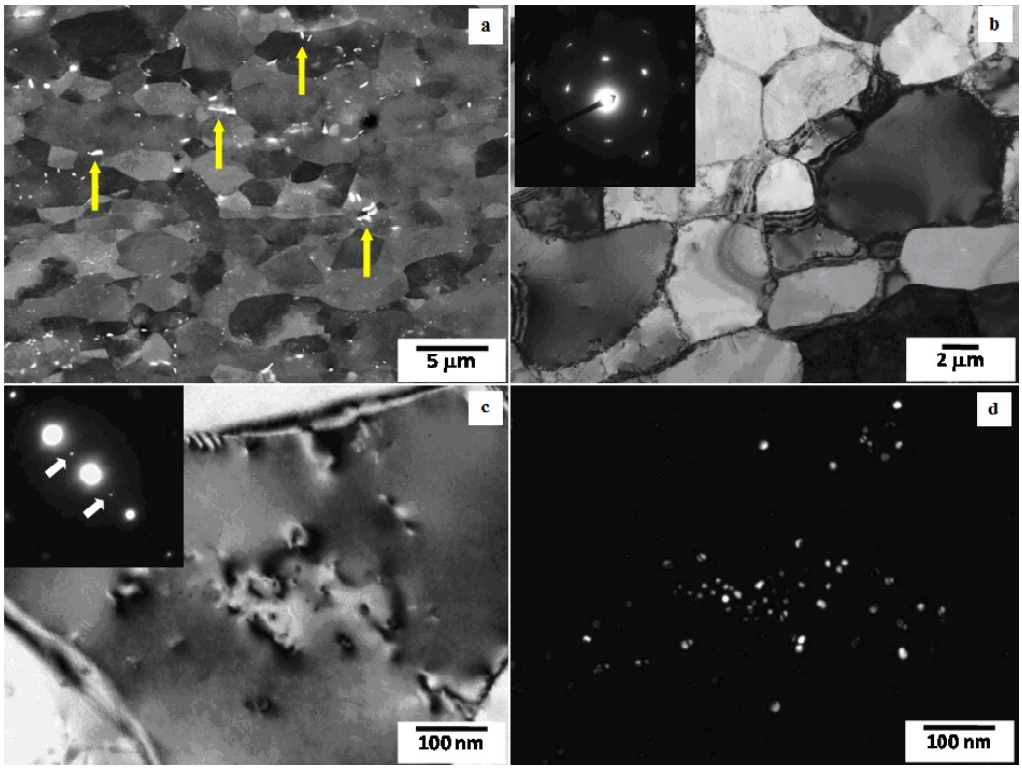

Fig. 3. (a, b) Microstructure of the as-received Al-0.4Mg-0.2Zr alloy: (a) SEM and (b) bright field TEM micrographs and corresponding SAED patterns. (c, d) Microstructure of the as-received Al-0.4Mg-0.2Zr alloy after HT at 385 °C, 120 h: (c) bright field TEM micrographs and corresponding SAED patterns showing superlattice resections due to the presence of Al_3Zr precipitates and (d) dark field TEM image.

which is shown in Fig. 3b, demonstrating the formation of a subgrain-type structure with grain boundaries exhibiting mostly low-angle misorientation. It shows single reflections located along circles with a strongly expressed azimuth scattering. These SAED patterns are typical of the materials with the low angle grain boundaries dominating in the microstructure.

The initial material microstructure also contains an insignificant (volume fraction below 1%) amount of intermetallic crystalline particles varying from 0.5 to 2 μm in size (marked by an arrow) (Fig. 3a). Both particles and subgrains are oriented along the rolling direction. The precision analysis showed the presence of Fe, Si, and Al particles in the material with a stoichiometric ratio of 2:3:8. The presence of particles in such a combination is typical of Al alloys always containing some amount of Fe and Si [41,47].

The microstructural analysis of rods processed by ÍT (annealing at 385 °C for 120 hours) revealed the formation of nanoscale Al_3Zr precipitates with a metastable $L1_2$ structure (Figs. 3c and 3d). A mean particle size constitutes 22±3 nm with an interparticle distance equal to ~70 nm and no considerable variations in a subgrain size, which is possibly caused by the substructure stabilization with Al_3Zr precipitates.

The observed microstructural changes in the alloy following the HT agree well with the variations in hardness and specific electrical resistance of the material (Fig. 3). The experimentally measured data on the material strength after the HT also fit the strength level of annealed 5005 alloy of the Al-Mg system with a similar Mg content (~ 0.8 wt.%) (Table 2) [45].

It should be noted that electrical resistivity measured experimentally in the alloy processed via HT (29.42 nΩm) differs from its estimated value. According to the Matthiessen's rule [48], contributions into total electrical resistivity of metallic materials can be summed up if they act independently. The resistivity of pure Al is 26.55 nΩm [47]. So, if assume that residual Zr content of 0.2 wt.% Zr in the alloy solid solution following HT at 385 °C (as stated in [16]) increases Al electrical resistivity by 0.08 nΩm, and Mg concentration of 0.4 wt.% remains the same, which increases the electrical resistivity of the alloy [40] by 2.24 nΩm, then the material total value should be 28.87 nΩm, which is somewhat below the experimental data (Table 2). The observed difference in experimental

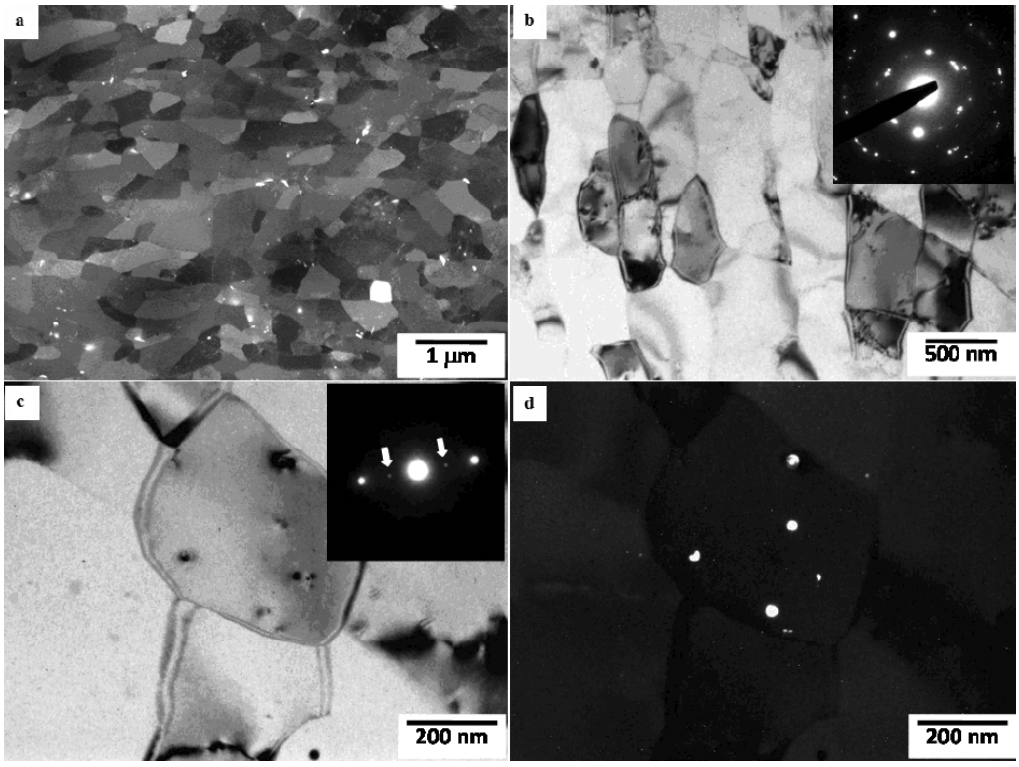

Fig. 4. Microstructure of Al-0.4Mg-0.2Zr alloy after ECAP-C processing: (a) SEM image, (b) bright field TEM image with corresponding SAED patterns taken from the longitudinal section; (c,d) bright field and dark field TEM images of nanoscale Al_3Zr precipitates, (c) corresponding SAED patterns showing superlattice resections formed by Al_3Zr precipitates.

Table 3. Results of the X-ray studies of the UFG Al alloy.

State	CSD, [nm]	$<\varepsilon^2>^{1/2}$, [%]	Lattice parameter, [Å]	ρ, [m^{-2}]
HT + 6 p ECAP-C at RT	141±6	0.1100±0.0001	4.0522±0.0001	9.4×10^{13}
ECAP-C + cold drawing	96±8	0.1500±0.0001	4.0523±0.0003	1.4×10^{14}
ECAP-C + cold drawing + anneal. at 230 °C, 1 h	161±1	0.0300±0.0003	4.0526±0.0002	2.3×10^{13}

and calculated electrical resistivity is possibly caused by the presence of impurities (Fe and Si) (Table 1), as well as nanoscale Al_3Zr precipitates in the alloy.

3.3. Structure and properties of the alloy processed via ECAP-C, cold drawing and annealing

The results of the microstructural studies of the rods subjected to 6 ECAP-C cycles at room temperature are shown in Fig. 4 and Table 3. The given treatment resulted in the formation of an UFG structure with a grain/subgrain size from 600 to 800 nm (Figs. 4a and 4b). Ultrafine grains are elongated along the shear plane, which is typical of Al-Mg alloys subjected to ECAP [33,49]. SAED patterns testify to the formation of a grain-type structure with grain boundaries exhibiting mostly high-angle misorientation, which can be seen in Fig. 4b [32,33], as well as proved by the findings in [39]. The authors of the research has established that ECAP of Al-0.13Mg (wt.%) at room temperature with an effective strain of 4 (like in the present study) resulted in the formation of UFG microstructure with a fraction of high-angle boundaries equal to 50%.

The microstructural analysis also shows that the morphology of Al_3Zr precipitates (Figs. 4a and 4d) is not affected by SPD processing.

According to the outcomes of X-ray analysis, the lattice dislocation density in samples after ECAP-C processing constituted 9.4×10^{13} m^{-2}, with a CSD size of 141 nm (Table 3).

Ultrafine grains processed as a result of ECAP-C become elongated along the axes of rods in the form of wire after cold drawing (Figs. 5a and 5c). The length of such grains extends up to 1 μm. In some grains, the formation of transverse sub boundaries can be observed (Fig. 5c). The wire microstructural analysis revealed an equiaxed shape of grains in rods cross section (Figs. 5b and 5d) with a size of grains varying from 100 to 400 nm, which agrees well with the width of grains elongated in the cross section (Figs. 5a and 5c). Similar UFG microstructure transformation was earlier observed in other UFG materials subjected to a cold drawing [27,50].

A microstructural analysis also showed that a cold drawing of the alloy resulted in the redistribution of nanoscale Al_3Zr precipitates, which were reoriented in a drawing direction. They also formed clusters in the form of lines (Figs. 5e and 5f), which is typical of semi-finished Al products obtained by extrusion/pressing [51].

According to X-ray analysis, additional drawing leads not only to grain refinement, but also to a considerable increase in dislocation density in the UFG alloy from 9.4×10^{13} m^{-2} to 1.4×10^{14} m^{-2} and, as a result, to the decrease in the coherent scattering region size from 141 to 96 nm (Table 3).

Table 2 shows strength, ductility and electrical conductivity in the alloy processed by ECAP-C and drawing. According to the experimental data obtained, the formation of an UFG microstructure in the studied material leads to both YS and UTS increase by 2 and 1.6 times, correspondingly. Also, an elongation to failure in samples processed via ECAP-C is decreased, especially its uniform components (Fig. 2), which is due to a quick tensile strain localization typical of UFG metals and alloys, including those Al-based [22].

A cold drawing results in an additional strengthening of the UFG alloy by ~30 %, which is caused both by a reduction of grain size (Fig. 5), and an increase in a dislocation density (Table 3). It is important that UFG wire has a relative elongation to failure above 2%, which meets the requirements to thermally stable conducting Al-based wire [14].

After a special annealing at 230 °C for 1 hour (recommended in [14] to determine the level of thermal stability in conducting Al alloys), the level of ultrafine grains in wire samples remained nearly the same, which can be explained by the presence of nanoscale Al_3Zr precipitates in the microstructure. At the same time, the annealing resulted in a considerable decrease in dislocation density, according to X-ray analysis (Table 3). These microstructural changes led to a decrease in UFG wire UTS from 267 to 245 MPa (Table 2), which is lower than 10%. The given strength degradation is

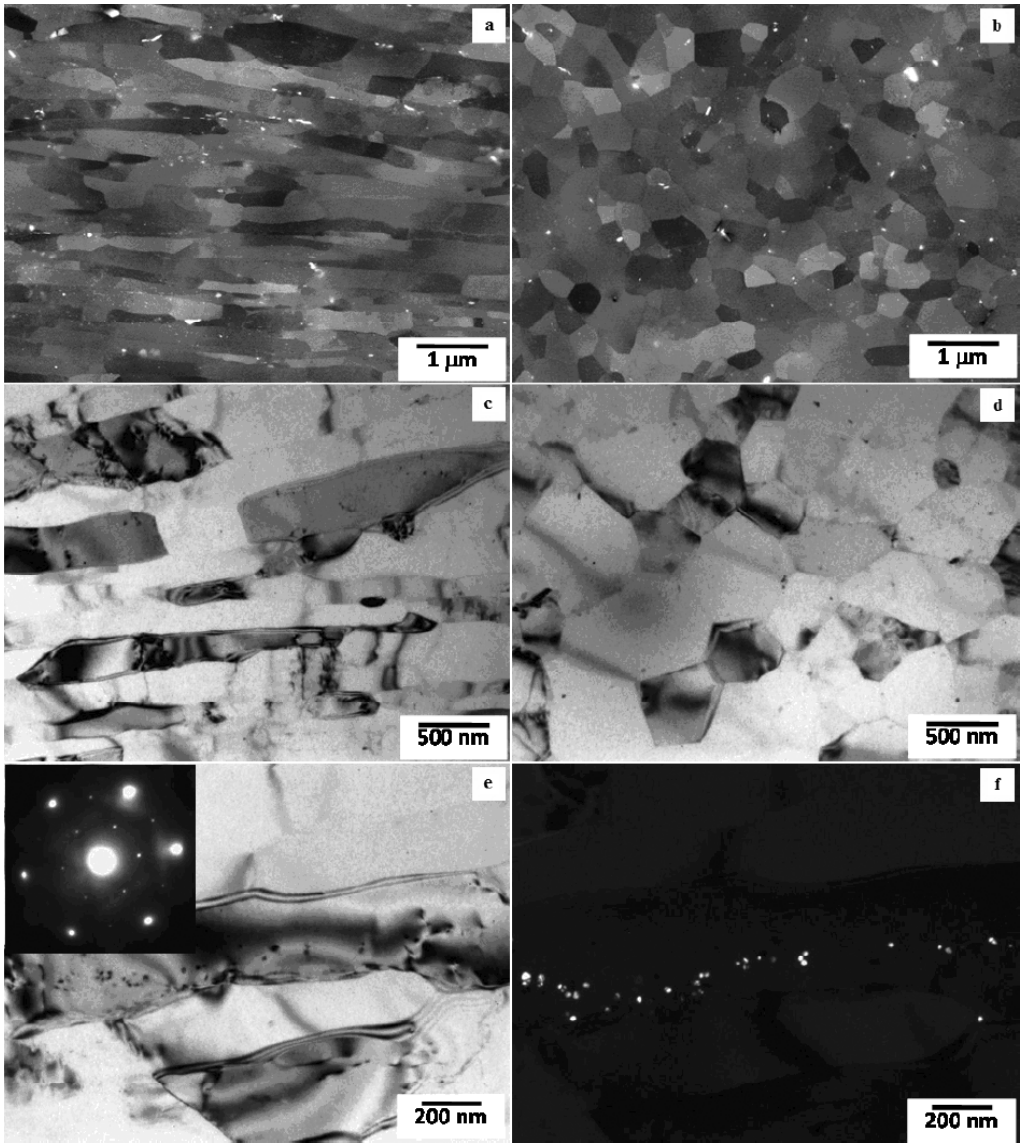

Fig. 5. Microstructure of Al-0.4Mg-0.2Zr alloy after ECAP-C processing and cold drawing: (a, c, e, f) on longitudinal section and (b, d) on transversal section. (a, b) SEM images, (c, d) bright field TEM images. (e) bright field TEM image showing nanoscale Al_3Zr precipitates and corresponding SAED patterns. (f) dark field TEM image showing nanoscale Al_3Zr precipitates.

acceptable after a short-time annealing at 230 °C for 1 hour for heat resistance alloys with a long-term service temperature not exceeding 150 °C [14].

A notable strength enhancement in the UFG alloy samples processed via ECAP-C and a cold drawing and remaining relatively high even after a special annealing is not accompanied by a considerable change of electrical conductivity (Table 2). This is conditioned by the fact that the electrical conductivity level in conducting alloys depends more on the concentration of alloying element atoms in a solid solution, than on such microstructural parameters as a dislocation density and a grain size [11-13,23,52,53]. The absence of any notable changes in the lattice parameter (Table 3) of the alloy after all types of treatment following the HT at 385 °C points that the concentration of Mg and Zr atoms in the Al alloy solid solution remains the same. Thus, it can be assumed that the increase in the alloy resistivity after ECAP-C and a cold drawing from 29.42 nΩm to 29.93 nΩm and 30.18 nΩm (Table 2), correspondingly, is conditioned by a grain size decrease only.

Comparing the properties of Al-0.4Mg-0.2Zr UFG wire with those of widely used and even promising thermally stable Al alloys (Table 2), it can be concluded that the selected studied material as well as the structural state processed by a TMT including

SPD, enable to get the best combination of strength (UTS=267 MPa), electrical conductivity (57.1% IACS), and heat resistance (up to 150 °C).

This study and the results of the earlier research [16-20,29] allow to state that both strength and heat resistance of Al-Mg-Zr alloys can be enhanced. One way is to increase the content of Zr to no less than 0.4 wt.% to additionally enhance the strength of the conducting alloy through precipitation hardening by increasing the volume fraction of the Al_3Zr nanoscale metastable precipitates. Besides, new high-efficient techniques based on ECAP-C [54,55] can lead to the formation of an UFG microstructure in the Al-Mg-Zr alloy for only 1 treatment cycle, which is extremely important for commercial scale production of new materials for All Aluminium Alloy Conductors.

5. CONCLUSIONS

The effect of a thermomechanical treatment including both annealing and deformation processing via ECAP-C and a cold drawing on the microstructure, strength, electrical conductivity, and heat resistance of the Al-0.4Mg-0.2Zr (wt.%) was studied. The following conclusions can be made:

1. The selected chemical composition and the TMT regime including SPD process result in the formation of an UFG microstructure with dislocation density of 1.4×10^{14} m^{-2} and nanoscale precipitation of Al_3Zr, with a mean size of 22 nm.
2. The processed UFG state leads to a considerable increase in UTS from 129 MPa to 267 MPa accompanied by an acceptable ductility (El. > 2%) and a good electrical conductivity (57.1% IACS).
3. The processed UFG alloy can be used at a service temperature of up to 150°C for a long time.
4. The UFG Al-0.4Mg-0.2Zr (wt.%) alloy opens great perspectives for electrical engineering due to its combination of enhanced strength and electrical conductivity and heat resistance as compared to well-known Al alloys of conventional and enhanced compositions. The further studies shall be aimed at the additional enhancement of strength and heat resistance of Al-Mg-Zr alloys by using additional enhancement of their nanostructural parameters.

ACKNOWLEDGMENTS

This work in its part addressing examinations of microstructure, mechanical properties and heat resistance was supported by the Russian Science Foundation (Project 14-29-00199) and in its part concerning studies of electrical conductivity was supported by the President of the Russian Federation grant № NSh-7996.2016.8 for leading scientific schools.

REFERENCES

[1] F. Kutner, *Aluminium – monograph, aluminium conductor materials* (Aluminium-Verlag GmbH, 1981).
[2] F. Kiessling, P. Nefzger, J.F. Nolasco and U. Kaintzyk, *Overhead power lines: Planning, Desing, Construction* (Springer-Verlag, Berlin, 2003).
[3] Sedat Karabay and F. Kaya Önder // *Electric Power Syst. Res.* **72** (2004) 179.
[4] Karabay Sedat // *Mater. Design* **27** (2006) 821.
[5] *Overhead Power Line Conductors—Bare Conductors of Aluminium Alloy with Magnesium and Silicon Content*, EN 50183:2002.
[6] T.G. Zhou, Z.Y. Jiang, J.L. Wen, H. Li and A.K. Tieu // *Mater. Sci. Eng.* A **485** (2008) 108.
[7] Y. Wuhua and L. Zhenyu // *Mater. Design* **32** (2011) 4195.
[8] E. Cervantes, M. Guerrero, J.A. Ramos and S.A. Montes // *Mater. Res. Soc. Symp. Proc.* **1275** (2010) 75.
[9] B. Smyrak, M. Gniełczyk, B. Jurkiewicz, T. Knych, K. Korzeń, M. Jabłoński, A. Mamala and A. Nowak // *Key Eng. Mater.* **682** (2016) 138.
[10] D. Tie, R. Guan, N. Guo, Z. Zhao, N. Su, J. Li and Y. Zhang // *Metals* **5** (2015) 648.
[11] M.Yu. Murashkin, I. Sabirov, V.U. Kazykhanov, E.V. Bobruk, A. Dubravina and R.Z. Valiev // *J. Mater. Sci* **48** (2013) 4501.
[12] R.Z.Valiev, M.Yu. Murashkin and I. Sabirov // *Scr. Mater.* **76** (2014) 13.
[13] M. Murashkin, A. Medvedev, V. Kazykhanov, A. Krokhin, G. Raab, N. Enikeev and R.Z. Valiev // *Metals* **5** (2015) 2148.
[14] *Thermal resistant aluminum alloy wire for overhead line conductors*, IEC 62004:2007.
[15] T. Horikoshi, H. Kuroda, M. Shimizu and S. Aoyama // *Hitachi Cable Rev.* **25** (2006) 18.
[16] T. Knych, M. Piwowarska and P. Uliasz // *Arch. Metal. Mater.* **56** (2011) Issue 3 685.
[17] N.A. Belov, A.N. Alabin and A.R. Teleuov // *Metal Sci. Heat Treat.* **53** (2012) 455.
[18] N.A. Belov, A.N. Alabin, I.A. Matveeva and D.G. Eskin // *Trans. Nonferrous Met. Soc. China* **25** (2015) 2817.
[19] *High-strength heat-resistant aluminium alloy, conductive wire, overhead wire and method of*

preparing the aluminium alloy, EP 0787811 A1 20.01.1997.
[20] W.W. Zhou, B. Cai, W.J. Li, Z.X. Liu and S. Yang // *Mater. Sci. Eng. A* **552** (2012) 353.
[21] *Aluminium-based heat-resistant conducting alloy*, Patent RU 2441090 C2.
[22] I. Sabirov, M. Murashkin and R.Z.Valiev // *Mater. Sci. Eng. A* **560** (2013) 1.
[23] M.Yu. Murashkin, I. Sabirov, X. Sauvage and R.Z. Valiev // *J. Mater. Sci.* **51** (2016) 33.
[24] G.J. Raab, R.Z. Valiev, T.C. Lowe and T.Y. Zhu // *Mater. Sci. Eng. A* **382** (2004) 30.
[25] C. Xu, S. Schroeder, P.B. Berbon and T.G. Langdon // *Acta Mater.* **58** (2010) 1379.
[26] I.P. Semenova, A.V. Polyakov, G.I. Raab, T.C. Lowe and R.Z. Valiev // *J. Mater. Sci.* **47** (2012) 7777.
[27] D.V. Gunderov, A.V. Polyakov, I.P. Semenova, G.I. Raab, A.A. Churakov, E.I. Gimaltdinova, I. Sabirov, J. Segurado, V.D. Sitdikov and I.V. Alexandrov // *Mater. Sci. Eng. A* **562** (2013) 128.
[28] T. Niendorf, A. Böhner, H.W. Höppel, M. Göken, R.Z. Valiev and H.J. Maier // *Mater. Design* **47** (2013) 138.
[29] N.A. Belov, A.N. Alabin, D.G. Eskin and V.V. Istomin-Kastrovskii // *J. Mater. Sci.* **41** (2006) 5890.
[30] Keith E. Knipling, David C. Dunand and David N. Seidman // *Acta Mater.* **56** (2008) 114.
[31] V.M. Segal // *Mater. Sci. Eng. A* **147** (1995) 157.
[32] T.G. Langdon, M. Furukawa, M. Nemoto and Z. Horita // *JOM* **52** (2000) 30.
[33] R.Z. Valiev and T.G. Langdon // *Prog. Mater. Sci.* **51** (2006) 881.
[34] M. Lutterotti, S. Matthies and H.R. Wenk, In: *Proceeding of the 12th International Conference on Textures of Materials (ICOTOM-12)* (Montreal, QC, Canada, 1999), p. 1599.
[35] L.K. Williamson and R.E. Smallman // *Phil. Mag.* **1** (1956) 34.
[36] *Method of measurement of resistivity of metallic materials*, IEC 60468:1974.
[37] Y. Iwahashi, Z. Horita, M. Nemoto and T.G. Langdon // *Metal. Trans. A*. **29** (1998) 2503.
[38] H. Hasegawa, S. Komura, A. Utsunomiya, Z. Horita, M. Furukawa, M. Nemoto and T.G. Langdon // *Mater. Sci. Eng. A* **265** (1999) 188.
[39] J. Gubicza, N.Q. Chinh, Z. Horita and T.G. Langdon // *Mater. Sci. Eng. A* **387–389** (2004) 55.
[40] P. Olafsson, R. Sandstrom and A. Karlsson // *J. Mater. Sci.* **32** (1997) 4383.
[41] L.F. Mondolfo, *Aluminium alloys: structure and properties* (Butterworths, London, 1976).
[42] P.B. Prangnell, J.S. Hayes, J.R. Bowen, P.J. Apps and P.S. Bate // *Acta Mater.* **52** (2004) 3193.
[43] M. Berta, P.J. Apps and P.B. Prangnell // *Mater. Sci. Eng. A* **410–411** (2005) 381.
[44] E.O. Hall // *Proc. Phys. Soc.* **64** (1951) 747.
[45] N.J. Petch // *J. Iron Steel Inst.* **174** (1953) 25.
[46] A.S. Friedman, T.V. Dobatkina and E.V. Muratova // *Izv. AN USSR, Metals* **1** (1992) 234.
[47] J.E. Hatch, *Aluminum: Properties and Physical Metallurgy* (ASM International: Metals Park, OH, USA, 1984).
[48] P.L. Rositter, *The Electrical Resistivity of Metals and Alloys* (Cambridge University Press: Cambridge, UK, 2003).
[49] B.P. Kashyap, P.D. Hodgson, Y. Estrin, I. Timokhina, M.R. Barnett and I. Sabirov // *Metall. Mater. Trans. A*. **40** (2009) 3294.
[50] G.S. Dyakonov, E. Zemtsova, S. Mironov, I.P. Semenova, R.Z. Valiev and S.L. Semiatin // *Mater. Sci. Eng. A* **648** (2015) 305.
[51] J.S. Robinson and W. Redington // *Mater. Chart.* **105** (2015) 47.
[52] Y. Miyajama, S. Komatsu, M. Mitsuha, S. Hata, H. Nakashima and N. Tsuji // *Phil. Mag*. **90** (2010) 4475.
[53] T.S. Orlova, A.M. Mavlyutov, A.S. Bondarenko, I.A. Kasatkin, M.Yu. Murashkin and R.Z. Valiev // *Phil. Mag*. **96** (2016) 2429.
[54] E. Fakhretdinova, G. Raab, O. Ryzhikov and R. Valiev // *IOP Conf. Ser.: Mater. Sci. Eng.* **63** (2014) 012037.
[55] E.I. Fakhretdinova, G.I. Raab and R.Z. Valiev // *Adv. Eng. Mater.* **17** (2015) 1723.